

Distribution and fractionation of Rare Earth Elements and Yttrium in suspended and bottom sediments of the Kali estuary, western India

S. Suja¹, Lina Fernandes*¹ and V. Purnachandra Rao^{1,2}

1- CSIR-National Institute of Oceanography, Dona Paula, Goa-403 004, India

2-Department of Civil Engineering, Vignan's University, Vadlamudi, Andhra Pradesh-522213, India.

* Corresponding author; E-mail: lfernandes@nio.org

Abstract

Concentrations of Rare Earth Elements (REE) and Yttrium (Y), and major metals (Al, Fe and Mn) were measured in suspended particulate matter (SPM) and bottom sediments of the Kali estuary, western India for their distribution and fractionation. The contents of SPM and metals in it were more uniform along the longitudinal transect during the monsoon. During the post- and pre-monsoons, low SPM in the upper/middle estuary coincided with high Fe and Mn and total-REE (Σ REE). But in the lower estuary SPM and its Σ REE content increased seaward while Fe and Mn decreased. The Y/Ho ratios decreased seaward during the monsoon but increased during the post-monsoon. Sm/Nd ratios were more uniform along the transect during monsoon but decreased marginally seaward in other seasons. The Post-Archean average Australian Shale (PAAS)-normalized REE patterns exhibited middle-REE (MREE) and heavy-REE (HREE) enrichment with positive Ce (Ce/Ce*), Eu (Eu/Eu*) and Y anomalies. The Ce/Ce* increased but Eu/Eu* decreased marginally seaward. The fine-grained sediments showed higher Σ REE and lower Y/Ho ratios than in coarse-grained sediments. The PAAS-normalized REE patterns of sediment were similar to that of SPM. The results revealed two processes, colloidal flocculation and co-agulation of metals in the low-salinity zone and an estuarine turbidity maximum (ETM) in the high salinity zone. Rare earths and yttrium (REY) in SPM and sediments primarily reflected the source rock composition than that of chemical weathering. Apart from physico-chemical processes, the mineralogy and grain size of sediments controlled the distribution and fractionation of REY in the estuary.

Key words: Rare earth elements, estuarine processes, chemical weathering, Kali estuary, India

Introduction

Estuaries are dynamic environments where complex biogeochemical processes modify the concentrations of dissolved trace metals and composition of suspended particulate matter (SPM) delivered by rivers to the ocean. Among trace metals, rare earth elements (REE) and yttrium (Y) exhibit a unique and coherent behavior and have been extensively used to identify source materials (Nesbitt 1979; Singh and Rajamani 2001; Xu et al. 2009; Jung et al. 2012), impact of chemical weathering (Nozaki et al. 1997; Feng 2010) and depositional processes (co-agulation, adsorption, desorption, flocculation, diagenetic mobilization and re-suspension) in rivers, estuaries and coastal systems. Studies on REE geochemistry of surface waters (fluvial, estuarine and marine) and sediments over the last three decades have identified different REE behavior such as rapid removal of Light REE (LREE) by adsorption (Elderfield et al. 1990; Sholkovitz and Szymczak 2000), oxidation of Ce relative to other REEs (Sholkovitz et al. 1994; Hannigan and Sholkovitz 2001), removal of dissolved REE and Y by scavenging on Fe-oxy-hydroxides (Byrne and Sholkovitz 1996; López-González et al. 2012), preferential adsorption of some REE on clay minerals in the presence of humic substances (Takahashi et al. 1998), fractionation of Y and Ho both at the weathering site and in river/sea water (Bau 1999; Nozaki et al. 1997, 2000) and, middle REE (MREE) enrichment and positive Ce anomaly in organic-rich estuarine sediments (Johannesson et al. 1996; Piper and Bau 2013). Studies on REE of SPM and bottom sediment further indicated, apart from source rock composition and weathering conditions, other factors, such as grain size, mineralogy and carbonate content in sediment could also contribute to the significant differences in the distribution and fractionation of REE (Yang et al. 2002; Feng 2010). The aim of this paper is to investigate seasonal variations in the distribution and fractionation of REE and Y in both SPM and bottom sediments along a longitudinal transect in the Kali estuary and identify the factors controlling their distribution.

Study area

Kali River, situated in the Karnataka state, west coast of India, originates in the Western Ghats (mountain regions), drains ~ 3,376 km² area (Manjunatha et al. 2001) and traverses ~180 km before discharging into the Arabian Sea. It begins as a south easterly flowing river but ends as a west flowing river in the Karwar Bay (Fig. 1). It has five major tributaries (Pandary, Tattihalla, Kaneri, Sakali and Vaki) and six dams/reservoirs built along its course (Supa, Bommanahalli, Kodsalli, Upper Kaneri, Tattihalla and Kadra reservoirs). The drainage area experiences tropical humid climate. Its annual rainfall is 3500 mm/year and the maximum rainfall occurs during the southwest monsoon (June – September). The annual river and sediment discharges into the estuary are reported to be ~6213 x 10⁶ m³ and ~0.7 x 10⁶ tons, respectively (Subramanian et al. 1987).

The catchment area of Kali River is dominated by greywackes in the upstream and granodiorite to tonalitic gneisses of the Dharwar Super Group in the downstream (Naqvi 2005). Manganese ore

deposits occur in the northern part. Limestones, dolomites, ultramafic rock complexes, orthoquartzites, argillites, banded magnetite/ hematite quartzites are minor rock types. Laterites cover the basic rock formations in the coastal region. We have investigated the estuarine part of the river along a transect of ~26 km (Fig. 1) from the mouth of the river, up to Kadra, beyond which is the Kadra dam. The Kali river estuary is partially mixed with an axial extension of ~26 km. The tides are semi-diurnal with an amplitude of ~2 m (Kumar et al. 2010). Mudflats are characteristic at the estuarine mouth and the lower estuary and play an important role in trapping sediments. Manjunatha et al. (1996, 2001) reported a few trace metals in soil profiles, SPM and bottom sediments of the Kali River estuary. They reported high manganese (Mn) content and related it to mining activities in the catchment area. In this paper we report the seasonal variations in SPM concentrations and distribution and fractionation of REE in both SPM and sediments.

Materials and Methods

Surface water samples were collected using a clean acid-washed plastic bucket and mechanized boat at ten stations along a transect of 26 km upstream from the mouth of the Kali estuary (Fig. 1). Samples were collected seasonally during the pre-monsoon (May 2012), monsoon (August 2012), post- monsoon (January 2013) seasons (months). Salinity of the water was measured, using 8400 Guildline Autosol Salinometer. For SPM measurements, 1.5 l of water were filtered through preweighed 0.40 μm polycarbonate membrane filter paper and the particles retained on the paper was dried at $<40^\circ\text{C}$ and weighed. SPM is expressed as milligram per liter.

For the geochemistry of the suspended matter, 20 l of water were filtered and dried. SPM was carefully removed from the polycarbonate membrane filter papers, accurately weighed and transferred into Teflon beakers. The samples were digested using an acid mixture of HF: HNO₃: HClO₄ in the proportion 6: 3: 1, kept overnight and then dried on a hot plate at 180°C. This procedure was repeated till the sample in the beaker was completely digested. The final residue was dissolved in 30 ml of 1:1 HNO₃. Subsequently, 1 ppm Rh solution was added as an internal standard and made up to the final volume. These aliquots were analyzed using Inductively-Coupled Plasma Optical Emission Spectrometer (ICP-OES; Agilent 700) for major elements and Inductively-Coupled Plasma Mass Spectrometer (ICP-MS; Thermo X series 2) for rare earth elements (REE) and Y concentrations in our laboratory. Table 1 shows the accuracy and reproducibility/ precisions of geochemical analyses with reference to MAG-1 (marine mud, United States Geological Survey, 1995). The accuracy was found to be better than $\pm 5\%$ and reproducibility/precision was $\pm 4\%$. Rare earth elements were divided into light REE (LREE: La-Nd), middle REE (MREE: Sm-Ho) and heavy REE (HREE: Er-Lu) following Rollinson (1993) and their ratios were calculated. Ce (Ce/Ce*) and Eu (Eu/Eu*) anomalies were calculated by normalizing with PAAS values, and using the following equations developed by Taylor and McLennan (1985).

Ce anomaly ($Ce/Ce^* = 3Ce_n / (2La_n + Nd_n)$), Ce_n , La_n and Nd_n are normalized values with respect to PAAS

Eu anomaly ($Eu/Eu^* = Eu_n / (Sm_n \times Gd_n)^{1/2}$), Eu_n , Sm_n and Gd_n are normalized values with respect to PAAS.

Bottom sediments were also collected, using Van Veen grab at the same ten stations where surface water samples were taken. Surface sediment was carefully peeled off by opening one flap of the grab and transferred into a polythene bag. Representative sub-samples were dried. The sand, silt and clay contents of the sediment were determined, following Folk (1968). Representative samples were powdered and major and trace metals of the powders were analyzed by following the above mentioned procedures.

Results

Salinity of the surface waters

For convenience of description of results the Kali estuary is divided into upper, middle and lower estuary as shown in Fig. 1. The salinity profile of the surface waters along transect stations is dependent on the season (Fig. 2A; Table 2). Salinity was low and uniform (0.04 -0.05) at stations in the upper/middle estuary and increased to a maximum of 3.5 in the lower estuary during the monsoon. The salinity values were low (<4) in the upper/middle estuary but increased gradually from 0.05 to 34.4 and from 0.06 to 34.8 along the transect stations during the post- and pre-monsoons, respectively.

Characteristics of SPM in the Kali estuary

Concentrations of SPM: Seasonal variations in the distribution of SPM along the transect stations are shown in Fig. 2A. The concentrations of SPM were more uniform at stations in the upper and middle estuary than in the lower estuary during the monsoon. The mean SPM concentrations were 14.8 mg/l, 13.3 mg/l and 15.2 mg/l in the upper, middle and lower estuary, respectively. During the post- and pre-monsoons, the SPM concentrations were low at river end stations (0.97 – 1.35 mg/l) but increased gradually seaward with its highest concentrations (up to 27.7 mg/l) in the lower estuary.

Concentrations of Al, Fe and Mn: Table 2 shows the seasonal variations in the major metals and rare earth elements and Y in SPM. The Al and Fe contents of SPM along the transect stations were higher than in the average suspended sediment of the World Rivers (ASSWR; Viers et al. 2009) and PAAS (Taylor and McLennan 1985). The Mn content of SPM (0.2-0.5 %) was 1-2 times higher than in ASSWR (0.2 %) during the monsoon. During the post- and pre-monsoons, the high Mn values in the upper/middle estuary (5.3-5.6%; Table 2) were 26-28 times higher than in ASSWR. The Al, Fe and Mn concentrations were nearly uniform along the transect stations during the monsoon. The Fe

and Mn of SPM were much higher at stations in the upper/middle estuary but decreased sharply seaward during the post- and pre-monsoons (Fig. 3A).

Total REE (Σ REE), Y/Ho and Sm/Nd ratios: The mean Σ REE of SPM of all the transect stations (Table 2) during the monsoon (154 μ g/g), post- (132 μ g/g) and pre-monsoons (130 μ g/g) were lower than in ASSWR (175 μ g/g) and PAAS (185 μ g/g). The mean Σ REE was always higher at stations in the lower estuary than in the upper estuary. Similar to that of Al, Fe and Mn, Σ REE showed abrupt fluctuations in the middle estuary and, relatively high Σ REE coincided with high SPM in the lower estuary (Fig. 2A). Correlation analysis carried out between REE and SPM showed no/weak correlation between Σ REE and SPM during the monsoon ($r=-0.34$, $p>0.1$) and post-monsoon ($r=0.15$, $p>0.1$) but moderate correlation during the pre-monsoon ($r=0.53$, $p>0.1$) (Fig. 4A). The Σ REE showed no correlation with Al and Fe during the monsoon ($r=0.04$, $p>0.1$; $r=0.14$, $p>0.1$) but exhibited moderate to strong correlation during the post- ($r=0.91$, $p<0.001$) and pre-monsoons ($r=0.74$, $p>0.01$). On the other hand, Σ REE and Mn were moderately correlated during the monsoon ($r=0.73$, $p>0.1$) and post-monsoon ($r=0.48$, $p>0.1$) and no correlation was seen during the pre-monsoon ($r=-0.02$, $p>0.1$) (Fig. 4). The LREE/HREE ratios (16.6 -21.4; Table 2) were much lower than in PAAS (24.66; Taylor and McClennan 1985) and decreased seaward during the monsoon, but increased during the post- and pre-monsoons. Yttrium (Y) and Ho displayed strong positive correlation ($r=0.9$; $p>0.001$) in all the seasons. The Y/Ho ratios (29.5 -31.1; Table 2) were higher than in ASSWR (25.3) and PAAS (27.4). This ratio decreased gradually seaward during the monsoon (Fig. 5A). The Y/Ho ratios were low in the upper estuary but increased sharply in the middle estuary and remained high in the lower estuary during the post-monsoon. The Y/Ho ratios were high and near uniform at river end stations, sharply decreased and remained low and uniform at sea end stations during the pre-monsoon (Fig. 5A). The Sm/Nd ratios (Table 2) maintained near uniform values along the transect stations during the monsoon but decreased marginally seaward during the post- and pre-monsoons (Fig. 5B).

REE patterns: The PAAS-normalized REE patterns of SPM displayed MREE- and HREE enrichment with positive Ce, Eu and Y anomalies (Y inserted between Dy and Ho) at every station and season (Fig. 6A). Ce anomaly (Ce/Ce^*) values were near uniform in the upper estuary but increased gradually seaward in the lower estuary in all the seasons (Fig. 7A). The Ce/Ce^* and Mn content of SPM showed no significant correlation during the monsoon but showed moderate inverse relationship during the post- and pre-monsoons (Fig. 7B). Eu anomaly (Eu/Eu^*) values showed minor variations along transect stations during the monsoon but decreased marginally seaward during the post- and pre-monsoons (Fig. 7C).

Bottom sediments in the Kali estuary

The sand, silt and clay contents of the sediments in the Kali estuary showed significant seasonal variations along the transect stations (Fig. 2B). The sediments were silty clay / sandy clay in the upper/middle estuary and sandy in the lower estuary during the monsoon. During the post-monsoon, sandy silt / silt occurred both at river end and sea end stations and sand at mid- stations. The sediments were sandy silt/clayey silt in the upper/middle estuary and sandy in the lower estuary during the pre-monsoon. The Fe and Mn in sediments of the upper/middle estuary (Table 3) were much higher than in PAAS. The Fe and Mn were high in the upper/middle estuary that decreased seaward (Fig. 3B). Al showed strong correlation with Fe and strong to moderate correlation with Mn in all seasons (Fig. 4B). The Σ REE of sediments varied widely from 17.7 to 173.6 $\mu\text{g/g}$ with relatively high values in clay- or silt-dominated sediments and low values in sandy sediments (Fig. 2B; Table 3). Σ REE showed strong positive correlation with Al and Fe of sediments in all the seasons (Fig. 4B), while exhibiting positive correlation with Mn during monsoon but moderate correlation during the post- and pre-monsoons. The Y and Ho and, Sm and Nd of sediments were positively correlated. The variations in Y/Ho ratios along the transect stations (29.3-32.3) followed that of dominant grain size fraction of the sediment with low ratios in clay/silt-dominated sediments and high ratios in sand-dominated sediments (Fig. 5A). The variations in Sm/Nd ratios of sediments (0.20 to 0.25) were not consistent except that this ratio was relatively high in fine-grained sediments at the river end stations (Fig. 5B).

The PAAS-normalized REE patterns of sediments were similar to that of SPM and displayed LREE-depletion and MREE- and HREE-enrichment patterns with positive Eu and Y anomalies at all the stations in all the seasons (Fig. 6B). The Ce/Ce* of sediments was positive during monsoon but a few sediments showed negative Ce anomaly in the post- and pre-monsoons (Fig. 7A). Ce/Ce* and Mn showed no correlation during the monsoon ($r=0.32$, $p>0.1$) but moderate correlation during the post- ($r=0.74$, $p>0.1$) and pre-monsoons ($r=0.71$, $p>0.1$) (Fig. 7B). The Eu/Eu* values remained similar in the upper / middle estuary and relatively high values in the lower estuary were associated with sandy sediments both during the monsoon and pre-monsoon (Fig. 7C).

Discussion

Record of estuarine sedimentary processes in the Kali estuary

The Kali River is a monsoonal river, which discharges runoff into the estuary mostly during the monsoon with very low discharge in other seasons. The salinity of the surface waters (Fig. 2A; Table 2) indicate largely river water dominance all along the estuary during the monsoon and, brackish waters (salinity <4) in the upper/middle estuary but estuarine/marine waters (increasing salinity seaward) in the lower estuary during the post- and pre-monsoons. The concentrations and composition of SPM reveal two important aspects of the estuary:

(a) The near uniform SPM concentrations (Fig. 2A), Fe and Mn (Fig. 3A) coinciding with very low salinity surface waters ($S < 0.04-0.05$) in the upper/middle estuary during the monsoon suggest strong freshwater flow dominated in this part of the estuary that seems to have minimized or diluted the process of flocculation. However, during the post- and pre-monsoons, the low salinity zone ($S < 0.04-4$) is associated with low SPM and high Al, Fe, Mn and ΣREE in the upper estuary or at the transition of upper/middle estuary (Figs. 2A and 3A) indicating prevalence of flocculation, wherein the dissolved and colloidal loads are influenced by co-agulation and then are scavenged onto the surfaces of metal oxides and clay particulates. Salinity increases gradually seaward both in post- and pre-monsoon. Despite low values, salinity shows an increasing trend from 0.04 to 4 in the upper/middle estuary. Several workers reported large scale removal of REE and other metals with increasing salinity in the low salinity zone by salt-induced coagulation of river colloids (Elderfield et al. 1990; Nozaki et al. 2000). High proportions of fine-grain size fractions of sediments in the upper estuary during the post-monsoon and in the upper/middle estuary during pre-monsoon (Fig. 2B) strongly suggest that the flocculants, by adsorbing onto clays, are being settled in bottom sediments.

(b) In the lower estuary, SPM concentrations are higher than in the upper estuary in all the seasons (Fig. 2A) and, increasing SPM concentrations seaward coincide with increasing salinity during the post- and pre-monsoons (Fig. 2A), indicating the occurrence of estuarine turbidity maximum (ETM) in the lower estuary. As the ETM is associated with high salinity waters it may have formed due to the combined influence of tidal and wind-induced currents. The narrow mouth of the bay might have led to high energy conditions that facilitated the re-suspension of bottom sediments. Very high SPM at station K2 that connects the bay and channel during the pre-monsoon (see Fig. 2A) supports this argument. The occurrence of ETM as a result of tidal processes that re-suspend sediments has been reported in several estuaries (Le Bris and Glamarec 1996; Kessarkar et al. 2010; Rao et al. 2011).

Factors controlling ΣREE , Y/Ho and Sm/Nd ratios in SPM and bottom sediment

ΣREE of SPM and sediments: The ΣREE of SPM largely depends on the chemical composition of its detrital inorganic particulates. The SPM comprising high Fe, Mn and Al; high ΣREE corresponding to high Mn and Fe in the upper estuary (Fig. 3A; Table 2) and moderate correlation of ΣREE with Mn during the monsoon (Fig. 4A) suggest that REE may have been derived from the hinterland rock formations; ferruginized laterites and Fe-Mn ore deposits in the drainage basin of the river. Manjunatha et al. (1996) reported very high Mn values in the estuary and implied its source to Mn ore deposits. High Fe and Mn in SPM also indicate the presence of Fe-Mn oxide-bound phases which can facilitate adsorption of large amounts of dissolved and colloidal REE that have been leached from the hinterland formations during intense chemical weathering. Despite chemical

weathering conditions and heavy monsoonal runoff into the estuary the ΣREE of SPM at river end stations is always lower than that of the World Rivers suggesting that the dissolved and colloidal load of REE and other elements may have quickly transferred to the coastal region because of the abundant and strong river flow during monsoon. Despite significantly less river supply during the post- and pre-monsoons, high Fe and Mn and ΣREE at the mixing zone in the middle estuary (Figs. 2A and 3A) indicate colloidal coagulation or dissolved pool of metals adsorbing onto suspended particles. On the other hand, the increase of ΣREE coinciding with increase in SPM content in the lower estuary (Fig. 2A) suggest that the ΣREE is controlled by the total SPM content, drawn from the re-suspension of bottom sediment by ETM. Similar observations are reported by Shynu et al (2013) in the Zuari River where high concentration of ΣREE in SPM was related to the occurrence of ETM zones. The variations in $\Sigma\text{REE}_{\text{SPM}}/\Sigma\text{REE}_{\text{Sed}}$ resembling that of $\Sigma\text{REE}_{\text{SPM}}$ (Fig. 2A) and, moderate inverse correlation between $\Sigma\text{REE}_{\text{SPM}}$ and $\Sigma\text{REE}_{\text{Sed}}$ ($r = -0.6$; $p > 0.001$) suggest that the bottom sediments supplied high SPM/REE to the water column.

The ΣREE of bottom sediment is usually dependent on grain size, heavy minerals and carbonate content (Yang et al. 2002). The wide variations in ΣREE of sediment are related to its grain size. High ΣREE in silty clays/clayey silts (Fig. 2B) and positive correlation of ΣREE with clay ($r = 0.54$; $p > 0.001$) and silt ($r = 0.64$; $p > 0.001$) contents and negative correlation with sand content ($r = -0.89$; $p > 0.001$) imply that the fine-grained particulates are better hosts for REE than sandy sediments. Strong correlation of ΣREE with Al, Fe and Mn of sediments (Fig. 4B) indicates REE are associated with alumino silicates (clay minerals) and Fe-Mn oxides/hydroxides. In general, clay minerals are important reservoirs of REE in riverine/estuarine and marine sediments and most of the REE reside in the clay mineral lattice whereas a small part is adsorbed onto clay mineral surfaces (Taylor and McLennan 1985; Coppin et al. 2002). Zhang et al. (2009) reported that the grain size of the sediment can exert strong influence on bulk REE and clay minerals are important reservoirs of REE in marine sediments. Carbonate content of the sediment is $< 1\%$. Heavy minerals may have contributed little to the ΣREE of sediment because heavy minerals concentrate in sand fraction of the sediments and sediments with high sand content showed very low ΣREE ($17 \mu\text{g/g}$; Fig. 2B). Therefore, ΣREE of sediment is largely controlled by fine-grained part of the sediment (clay and silt) in this estuary.

Y/Ho ratios of SPM and sediments: The positive correlation of Y and Ho with high level of significance ($p > 0.001$) in both SPM and sediment implies their similar geochemical behavior. Fractionation of Y and Ho, however, occurs during weathering in river and estuaries (Bau et al. 1995) and predominantly in the oceans (Nozaki et al. 1997). Higher Y/Ho ratios in SPM (29.5 -31.1; Table 2) and sediment (29.3-32.3; Table 3) than that of average CI chondrite (27.3; Barrat et al. 2012) and PAAS (27.4; McLennan 1989) indeed suggest that SPM and sediment contain a mixture

of detrital particulates from different sources and also plausible fractionation of Y/Ho ratio during weathering and transportation from river to estuary. High Y/Ho ratios of SPM/sediment indicate their greater mobility and higher loss of Ho to solution than Y during weathering. Careful examination shows that the slight decrease in Y/Ho ratios coincide with slight decrease in Fe and Mn concentrations in SPM, very low and uniform salinities (0.04 and 0.05) and near similar SPM concentrations during the monsoon (Figs. 2A, 3A and 5A). Similarly, the sharp rise in Y/Ho ratios coincide with rise in salinity from 0.05 to 12.0 and increase in Fe and Mn concentrations during the post monsoon (Figs. 3A and 5A). Thus, the decrease / increase in Y/Ho ratios is more related to the content of Fe and Mn, probably ore material at low salinities. The low and near uniform Y/Ho ratios associated with high salinities ($S > 32-34.5$) at seaward stations during pre-monsoon (Fig. 5A) may have been due to differences in complexation behavior between Y and Ho with inorganic (dicarbonate) and organic ligands on particulate matter. It is well known that Ho is scavenged twice faster than Y and adheres to the particulate matter at seawater salinities (Feng 2010). Ji et al. (2004) suggested marine particle reactivity of Y is considerably lower than its neighboring elements. Therefore, high adsorption of Ho onto particulates results in low Y/Ho ratios at seaward locations. On the other hand, relatively low Y/Ho ratios in clay or silt-dominated sediment and high ratios in sand-dominated sediments (Fig. 2B; Fig. 5A) suggest the composition of particulates and reactivity and scavenging of Ho onto the surfaces of clay particulates resulted in changes in Y/Ho ratios.

Sm/Nd ratios of SPM and sediments: The strong correlation between Sm and Nd ($p > 0.001$) suggest their similar geochemical behavior. The near uniform or marginal decrease in Sm/Nd ratios in SPM (0.20 to 0.22; Table 2; Fig. 5B) along transect stations of the estuary indicate decrease in source material away from the source and less influence of salinity and SPM content on this ratio. The Sm/Nd ratio of sediments (0.17 to 0.25; Table 3; Fig. 5B) are higher than that of PAAS (0.16) but lower than that of average CI chondrite (0.33; Barrat et al. 2012) suggesting that this ratio is influenced by mineral constituents (Viers and Wasserburg 2004). Feldspars contain high Nd. As feldspars are easily weathered to clays the Sm/Nd ratios would be low in clay-dominated sediments. The Sm/Nd of the Fe-Mn ore deposits is 0.27 (Prajith et al., 2015) while that of greywacke is 0.18 (Devaraju et al. 2010). Since ore deposits are present in the drainage basin and greywackes in the upper/middle estuary, the Sm/Nd may be influenced by them. Sandy sediments contain relic grains transported from hinterland that exhibit high Sm/Nd ratios. Therefore, the Sm/Nd ratio of sediment is controlled by source rock, clay content, ore material and relic grains. Sharp changes in Sm/Nd ratios (low as well as high ratios) in sand-dominated sediments (Fig. 5B) are difficult to explain, but may be controlled by different proportions of mineral constituents and ore material.

Controls on REE composition in SPM and bottom sediments

The low LREE/HREE and LREE/MREE ratios (Tables 2 and 3) and, MREE- and HREE-enriched REE patterns in both SPM and sediments of Kali estuary (Figs. 6A and B) are in contrast with that of

the suspended matter of the World Rivers (Yang et al. 2002) and estuarine sediments (Sholkovitz and Szymczak 2000), which exhibit LREE enrichment. Source rocks in the drainage basin are dominated by pre-cambrian granodiorite to tonolite gneisses, mafic-ultramafic complexes, greywackes and ore deposits of Fe and Mn. The PAAS-normalized REE patterns of greywackes, gneissic rocks and Fe-Mn ores (inserted in Fig. 6A and 6B) exhibit LREE-depleted, MREE- and HREE-enriched patterns with positive Eu anomaly in gneisses (Dhondial et al. 1987; Dessai et al. 2009) or Eu and Y anomalies (Bau and Dulski 1996) in greywackes (Devaraju et al. 2010) or Fe-Mn ores. As these formations are covered by laterites and subjected to chemical weathering one would expect the preferential solution of HREE from the top of weathering profile leaving a residue with relative LREE-enrichment. The clay-sized residue of the sediment would therefore be LREE-enriched relative to the source rocks. Moreover, SPM and sediments contain high Fe and Mn (Tables 2 and 3). Fe- and Mn oxy-hydroxides are known to provide active sites for adsorption of LREE (Marmolejo- Rodrigues et al. 2007) and MREE (Johannesson et al. 1999). In other words, one would expect more LREE and to certain extent MREE enrichment in SPM/sediment. The LREE-depleted and MREE- and HREE-enriched patterns (Fig. 6 A and B) therefore suggest that the REE composition of SPM/sediment is controlled by source rock composition rather than weathering. Since the REE patterns of SPM/sediment exhibit low Ce and Y anomalies (Fig. 6) compared to that of ore deposits (see inset in Fig. 6A) it is likely that these patterns are the result of relatively high degree of chemical weathering in the drainage basin, which promotes the mobility of MREE and HREE and would lead to their relative enrichment in SPM and sediment. It is also possible that the LREE-enriched, fine-grained, clay material transferred to the estuary, after weathering from the parent rock, may have been washed away periodically due to particle size sorting under high energy conditions of the estuary. Since both SPM and bottom sediment exhibit similar REE patterns we suggest that the influence of source rock is much greater than the chemical weathering.

Ce (Ce/Ce*) and Eu (Eu/Eu*) anomalies in SPM and bottom sediments

Ce is usually fractionated relative to other REE in estuaries and results in negative Ce/Ce* in the waters and positive Ce/Ce* in the underlying sediments. This is because the dissolved Ce³⁺ is oxidized to Ce⁴⁺ in the estuarine mixing zone and Ce⁴⁺ is rapidly removed to the sediment by scavenging onto clay particulates. The consistent positive Ce/Ce* in SPM (Fig. 7A) represents its inheritance from greywackes or ore deposits. The seaward increase in Ce/Ce* in the lower estuary corresponds to the increase in both SPM and Σ REE (Figs. 2A and 7A), that arose from the re-suspension of bottom sediments by ETM. Therefore, the seaward increase of Ce/Ce* is simply coincidental with increase of SPM in the lower estuary. Ce and Mn are redox sensitive elements and moderate correlation was observed between Ce/Ce* and Mn during the monsoon (Fig. 7B). However, the inverse correlation between Ce/Ce* and Mn during the post- and pre-monsoons (Fig. 7B) suggests that Ce may have responded to estuarine turbidity, but not Mn, being heavier.

Hannigan et al. (2010) and Shynu et al. (2013) reported that Ce responds more to physical mixing and particle settling. On the other hand, the sediments exhibit positive Ce/Ce* anomaly during the monsoon and slight negative Ce/Ce* during the post- and pre-monsoons (Fig. 6B). Bau and Duski (1996) suggested that the anomaly values would be significant if Ce/Ce* >1.05 or <0.95. Very few sediment samples showed such high (>1.05) or low (<0.95) Ce/Ce* values (Table 3). Further, the slight negative Ce anomaly could be due to low analytical precision for La and Ce compared to other REE, using ICP-MS method (Möller et al., 1992). Since increased Ce/Ce* in SPM corresponds to depleted Ce/Ce* in sediments (Fig. 7A) the slight negative Ce/Ce* could also be due to the re-suspension of very fine-grained bottom sediments.

Positive Eu/Eu* in both SPM and sediment (Fig. 7C) may have been inherited from parent rocks and ore deposits that characterized them. Ce/Ce* and Eu/Eu* responded differently in SPM, the former increased whereas the latter decreased seaward. The variations in Eu/Eu* in SPM along the transect stations, however, resembled that of Sm/Nd (Fig. 7C and 5B). These suggest that the seaward decrease of Eu/Eu* in SPM may be related to decreasing source material but not to SPM content and/or physical mixing. Similar to that of Nd, Eu is enriched in K-feldspar, greywacke and Fe-Mn ore material (see inset in Fig. 6A). High Eu/Eu* values associated with sandy sediments or silty sediments at seaward stations (Fig. 7C and Fig. 2B) may suggest that the mineral constituents (detrital material and ore material from hinterland) associated with sediments controlled the variations in Eu/Eu*.

Conclusions

Seasonal distribution of REE in SPM and bottom sediment along a longitudinal transect in the Kali estuary shows near uniform distribution of SPM and metals along transect during monsoon and increased SPM and Σ REE in the lower estuary during the post- and pre-monsoons. PAAS-normalized REE patterns show MREE- and HREE enrichment with positive Ce/Ce*, Eu/Eu* and Y anomaly in both SPM and sediment. Our results indicate flocculation of colloids and their adsorption onto suspended particulates and co-agulation of metals in low-salinity zone and estuarine turbidity maximum (ETM) in high salinity zone. The composition of REE is controlled by source rocks. The Y/Ho ratios of SPM/sediment largely depend on the composition of detrital particulates and nature of sediments. The Sm/Nd ratio and Eu anomaly depend on mineral constituents and grain size of sediments.

Acknowledgments

We thank the Director, National Institute of Oceanography, Goa for facilities. Research fellowship for S. Suja was supported by the Institutional Projects (PSC0105 and PSC0106). Drs. Pratima Kessarkar and Arti Tomar participated in the field trip to Kali estuary and guided Suja at various stages in the laboratory work. Drs Parthiban and Siby Kurian are thanked for the metal and REEs

analyses. This work was funded by CSIR-Ocean Finder Program (PSC0105). This is NIO contribution

References

Barrat Jean-Alix, Zanda B, Moynier F, Bollinger C, Liorzou C, Bayon G (2012) Geochemistry of Cl chondrites: Major and trace elements, and Cu and Zn Isotopes. *Geochim Cosmochim Acta* 83: 79-92.

Bau M (1999) Scavenging of yttrium and rare earths precipitating iron oxyhydroxide: experimental evidence for Ce oxidation, Y-Ho fractionation and lanthanide tetrad effects. *Geochim Cosmochim Acta* 63: 67-77.

Bau M, Dulski P (1996) Distribution of yttrium and rare-earth elements in the Penge and Kuruman iron-formations, Transvaal Supergroup, South Africa. *Precamb Res* 79: 37-55.

Bau, M, Dulski, P, Möller, P (1995) Yttrium and holmium in South Pacific seawater: vertical distribution and possible fractionation mechanisms. *Chem Erde* 55: 1-15.

Byrne RH, Sholkovitz ER (1996) Marine chemistry and geochemistry of the lanthanides. In: Gschneider Jr. KA and Eyring L (editors), *Handbook on the physics and chemistry of rare earths* 23: 497-593.

Coppin F, Berger G, Bauer A, Castet S, Loubet M (2002) Sorption of lanthanides on smectite and kaolinite. *Chem Geol* 182: 57-68.

Dessai AG, Arolkar DB, French D, Viegas A, Viswanath TA (2009) Petrogenesis of the Bondla layered mafic-ultramafic complex, Usgaon, Goa. *J Geol Soc India* 73: 697-714.

Devaraju TC, Sudhakara TL, Kaukonen RJ, Viljoen, RP, Alapieti TT, Ahmed SA, Sivakumar S (2010) Petrology and geochemistry of greywackes from Goa-Dharwar sector, western Dharwar Craton: Implications for volcanoclastic origin. *J Geol Soc India* 75(3): 465-487.

Dhondial DP, Paul DK, Sarkar A, Trivedi JR, Gopalan K, Potts PJ (1987) Geochronology and geochemistry of the Precambrian granitic rocks of Goa, SW India. *Precamb Res* 36: 287-302.

Elderfield H, Upstill-Goddard R, Sholkovitz ER (1990) The rare earth elements in rivers, estuaries and coastal seas and their significance to the composition of ocean water. *Geochim Cosmochim Acta* 54: 971-991.

Feng J (2010) Behaviour of rare earth elements and yttrium in ferromanganese concretions, gibbsite spots, and the surrounding terra rossa over dolomite during chemical weathering. *Chem Geol* 271: 112-132.

Folk RL (1968) *Petrology of sedimentary rocks*, Hemphils, Drawer's M. University station, Austin, Texas, 170.

Hannigan RE, Sholkovitz ER (2001). The development of middle rare earth element enrichments in freshwaters: weathering of phosphate minerals. *Chem Geol* 175: 495-508.

Hannigan RE, Dorval E, Jones C (2010) The rare earth element chemistry of estuarine surface sediments in the Chesapeake Bay. *Chem Geol* 272: 20-30.

Ji H, Wang S, Ouyang Z, Zhang S, Sun C, Liu X, Zhou D (2004). Geochemistry of red residual underlying dolomites in karst terrains of Yunnan–Guizhou Plateau II. The mobility of rare earth elements during weathering. *Chem Geol* 203: 29–50.

Johannesson KH, Lyons WB, Yelken MA, Gaudette HE, Stetzenbach KJ (1996) Geochemistry of the rare-earth elements in hypersaline and dilute acidic natural terrestrial waters: complexation behavior and middle rare-earth element enrichments. *Chem Geol* 133: 125-144.

Johannesson KH, Zhou X (1999) Origin of middle rare earth element enrichments in acid waters of a Canadian High Arctic lake. *Geochim Cosmochim Acta* 63: 153-165.

Jung HS, Lim D, Choi JY, Yoo HS, Rho KC, Lee HB (2012) REE compositions of core sediments from the shelf of the South sea, Korea; their controls and origins. *Cont Shelf Res* 48: 75-86.

Kessarkar PM, Rao VP, Shynu R, Mehra P, Viegas BE (2010) The nature and distribution of particulate matter in the Mandovi estuary, Central West Coast of India. *Estuar and Coast* 33: 30-44.

Kumar VS, Dora GU, Philip S, Pednekar P, Singh J (2010) Variations in tidal constituents along the nearshore waters of Karnataka, west coast of India. *J Coast Res* 27(5): 824-829.

Le Bris H, Glemarec M (1996) Marine and brackish ecosystems of south Brittany (Lorient and Vilaine Bays) with particular reference to the effect of the turbidity maxima. *Estuar Coast Mar Sci* 42: 737-753.

López-González N, Borrego J, Carro B, Grande JA, De la Torre M, Lalente T (2012) Rare-earth element fractionation patterns in estuarine sediments as a consequence of acid mine drainage: A case study in SW Spain. *Boletín Geológico y Minero* 123: 55-64.

Manjunatha BR, Balakrishna K, Shankar R, Thiruvengadasami A, Prabhu RK, Mahalingam TR, and Iyengar MAR (1996) The transport of elements from soils around Kaiga to the Kali river, southwest coast of India. *Sci Total Environ* 191: 109-118.

Manjunatha B, Balakrishna K, Shankar R, Mahalingam T (2001) Geochemistry and assessment of metal pollution in soils and river components of a monsoon-dominated environment near Karwar, southwest coast of India. *Environ Geol* 40: 1462-1470.

Marmolejo-Rodriguez AJ, Prego R, Meyer-Willerer A, Shumilin E, Sapozhnikov D (2007) Rare earth elements in iron oxy-hydroxide rich sediments from the Marabasco River-Estuary system. *J Geochem Explor* 94: 43-51.

Möller P, Dulski P, Luck J (1992) Determination of rare earth elements in seawater by Inductively coupled plasma-mass spectrometry. *Spectrochim Acta* 478: 1379-1382.

Naqvi SM (2005) *Geology and Evolution of the Indian Plate (from Hadean to Holocene 4 Ga to 4 Ka)*. Capital Publishing Company, New Delhi 450.

Nesbitt HW (1979) Mobility and fractionation of rare earth elements during weathering of a granodiorite. *Nature* 279, 206.

Nozaki Y, Zhang J, Amakawa H (1997) The fractionation between Y and Ho in the marine environment. *Earth and Planet Sci Lett* 148: 329-340.

Nozaki Y, Lerche D, Alibo DS, Snidvongs A (2000) The estuarine geochemistry of rare earth elements and indium in the Chao Phraya River, Thailand. *Geochim Cosmochim Acta* 64: 3983-3991.

Piper DZ, Bau M (2013) Normalized rare earth elements in water, sediments, and wine: identifying sources and environmental redox conditions. *Am J Anal Chem* 2013.

Prajith A, Rao VP, Kessarkar PM (2015) Controls on the distribution and fractionation of yttrium and rare earth elements in core sediments from the Mandovi estuary, western India. *Cont Shelf Res* 92: 59-71.

Rao, VP, Shynu R, Kessarkar PM, Sundar D, Michael GS, Narvekar T, Blossom V, Mehra P (2011) Suspended sediment dynamics on a seasonal scale in the Mandovi and estuaries, central west coast of India. *Estuar Coast Shelf Sci* 91: 78-86.

Sholkovitz ER, Szymczak R (2000) The estuarine chemistry of rare earth elements: comparison of the Amazon, Fly, Sepik and the Gulf of Papua systems. *Earth Planet Sci Lett* 179: 299-304.

Sholkovitz ER, Landing W, Lewis B (1994) Ocean particle chemistry: The fractionation of rare earth elements between suspended particles and seawater. *Geochim Cosmochim Acta* 58: 1567-1579.

Shynu R, Rao VP, Parthiban G, Balakrishnan S, Narvekar T, Kessarkar PM (2013) REE in suspended particulate matter and sediment of the Zuari estuary and adjacent shelf, western India: Influence of mining and estuarine turbidity. *Mar Geol* 346: 326-342.

Singh P, Rajamani V (2001) REE geochemistry of recent clastic sediments from the Kaveri floodplains, Southern India: Implication to source area weathering and sedimentary processes. *Geochim Cosmochim Acta* 65: 3093-3108.

Takahashi Y, Minai Y, Kimura T, Tominaga T (1998) Adsorption of europium (III) and americium (III) on kaolinite and montmorillonite in the presence of humic acid. *J Radioanal and Nuclear Chem* 234: 277-282.

Taylor SR, McLennan SM (1985) *The Continental Crust: its Composition and Evolution*. Blackwell, Oxford, 312.

Viers J, Dupre B, Gaillardet J (2009) Chemical composition of suspended sediments in World Rivers: New insights from a new database. *Sci Total Environ* 407: 853-868.

Viers J, Wassenburg GJ (2004) Behavior of Sm and Nd in a lateritic soil profile. *Geochim Cosmochim Acta* 68: 2043–2054.

Xu Z, Lim D, Choi J, Yang S, Jung H (2009) Rare earth elements in bottom sediments of major rivers around the Yellow Sea: implications for sediment provenance. *Geo-Marine Lett* 29: 291-300.

Yang SY, Jung HS, Choi MS, Li CX (2002) The rare earth element compositions of the Changjiang (Yangtze) and Huanghe (Yellow) river sediments. *Earth Planet Sci Lett* 201: 407-419.

Zhang H, Zhang WX, Chang FQ, Yang LQ, Lei GL, Yang MS, Pu Y, Lei YB (2009) Geochemical fractionation of rare earth elements in lacustrine deposits from Qaidam basin. *Science in China series D: Earth Sci* 52: 1703-1713.

Figure captions

Fig. 1. Sample locations in the Kali estuary, west coast of India. Zones of upper estuary, middle estuary and lower estuary are also marked.

Fig. 2. (A) Seasonal distribution profiles of suspended particulate matter (SPM; histograms), salinity, ΣREE of SPM and $\Sigma\text{REE}_{\text{SPM}}/\Sigma\text{REE}_{\text{sed}}$ along transect stations in the Kali estuary. (B) Seasonal distribution in the sand, silt and clay percentage and ΣREE of bottom sediments along transaction stations in the Kali estuary. To distinguish the samples of upper estuary (UE) from lower estuary (LE) the samples in middle estuary (ME) are shaded.

Fig. 3. Seasonal variations in the concentrations of Al, Fe, Mn and ΣREE in (A) SPM and (B) bottom sediments along transect stations in the Kali estuary.

Fig. 4. (A) Correlation plots of ΣREE of SPM with SPM content, Al, Fe and Mn concentrations of SPM. (B) Correlation plots of ΣREE of bottom sediments with its Al, Fe and Mn content. Correlation plot of Al vs. Mn in bottom sediments is also shown.

Fig. 5. Seasonal variations in (A) Y/Ho ratio and (B) Sm/Nd ratio of SPM and bottom sediments along transect stations in the Kali estuary.

Fig. 6. PAAS-normalized REE patterns of (A) SPM and (B) bottom sediments in the transect stations. PAAS-normalized REE patterns of gneissic rock, iron ore (Prajith et al. 2015) and greywackes (Devaraju et al. 2010), are also shown.

Fig. 7. (A) Seasonal variations in Ce anomaly (Ce/Ce^*) in SPM and bottom sediments along transect stations. Seasonal variations in Mn content of SPM along transect is also shown. (B) The plot of Ce/Ce^* with Mn content of SPM and bottom sediment during monsoon, post- and pre-monsoons. (C) Seasonal variations in the Eu anomaly (Eu/Eu^*) in SPM and bottom sediments along transect stations in the Kali estuary.

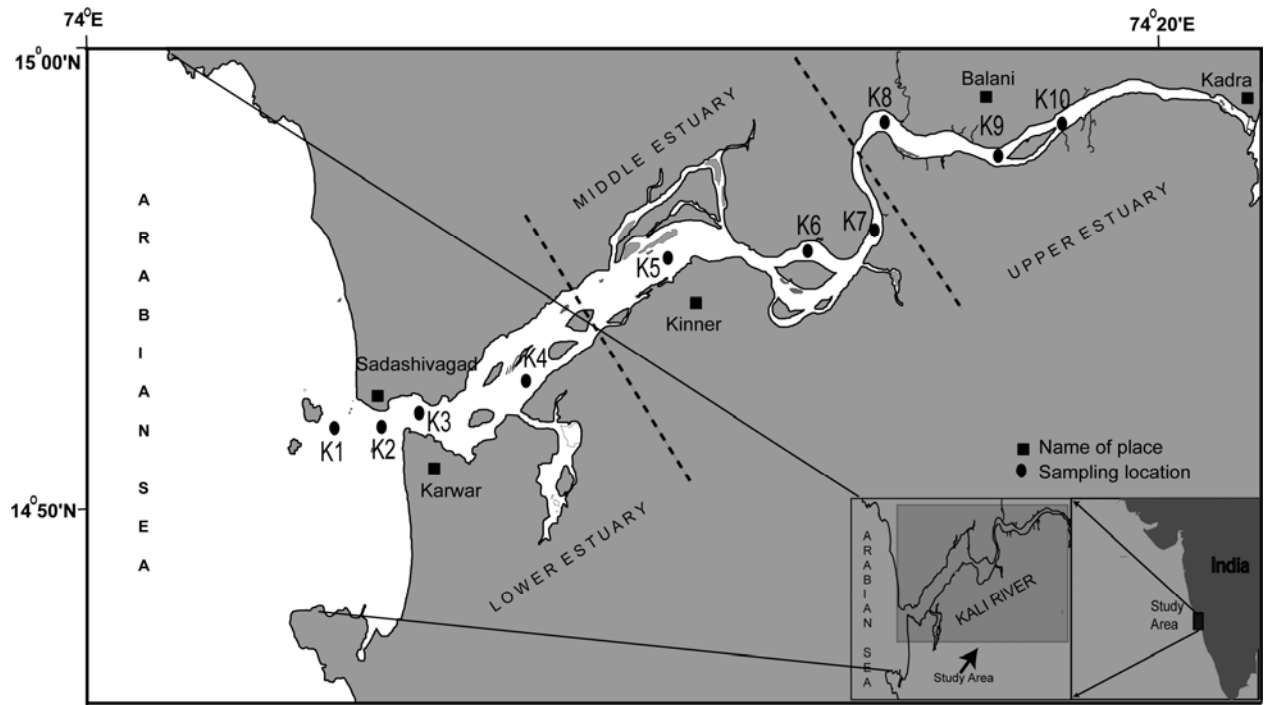


Figure. 1.

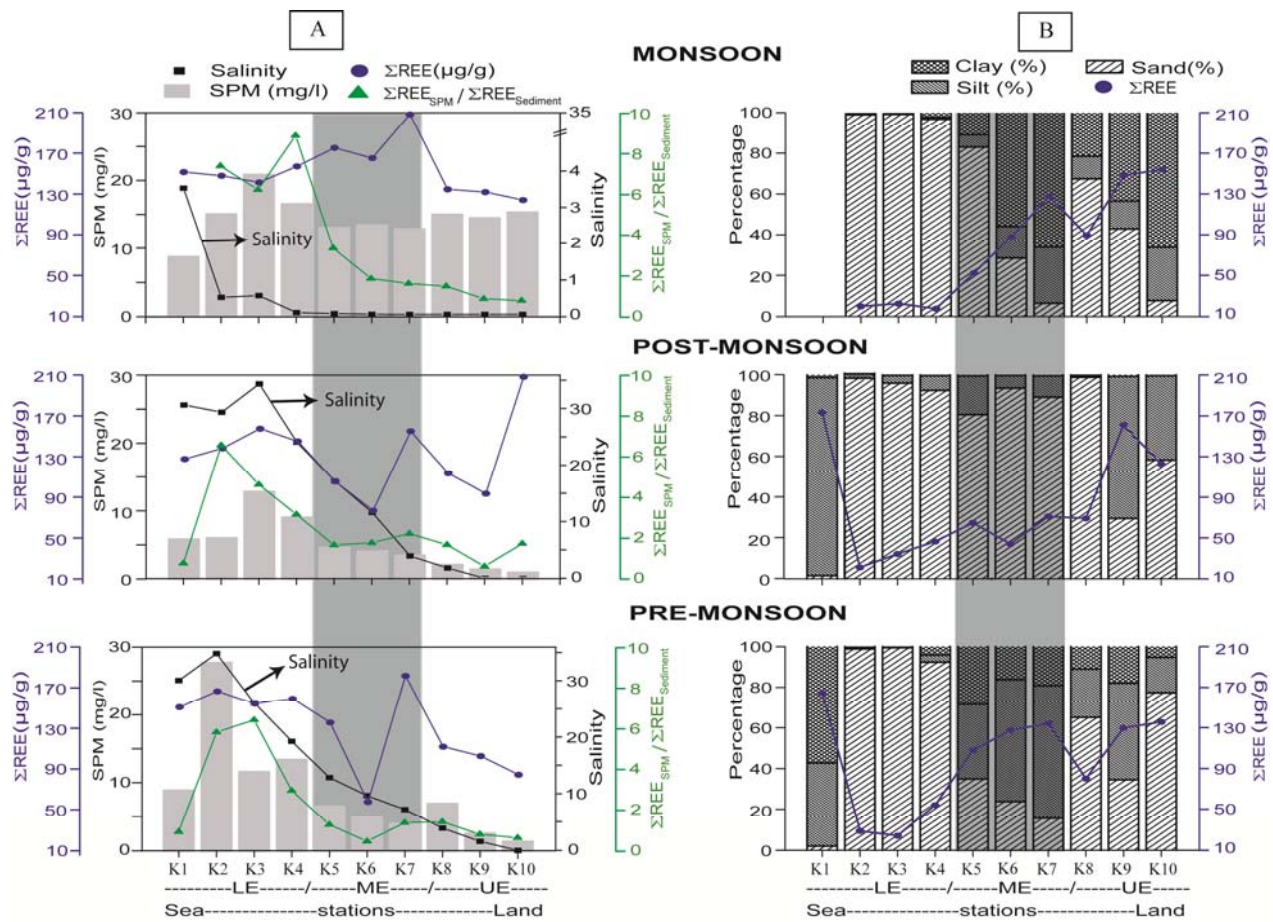


Figure. 2

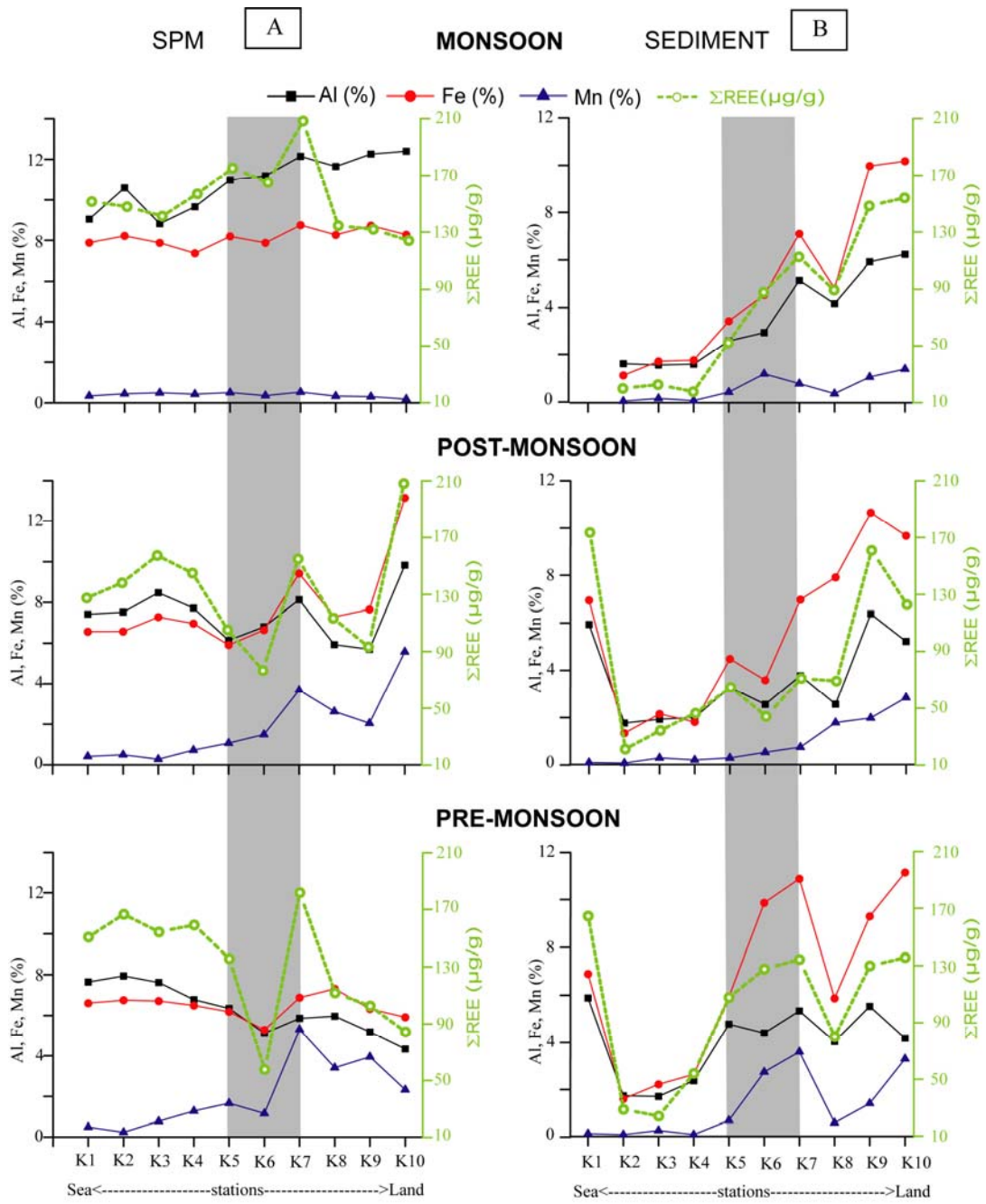


Figure. 3

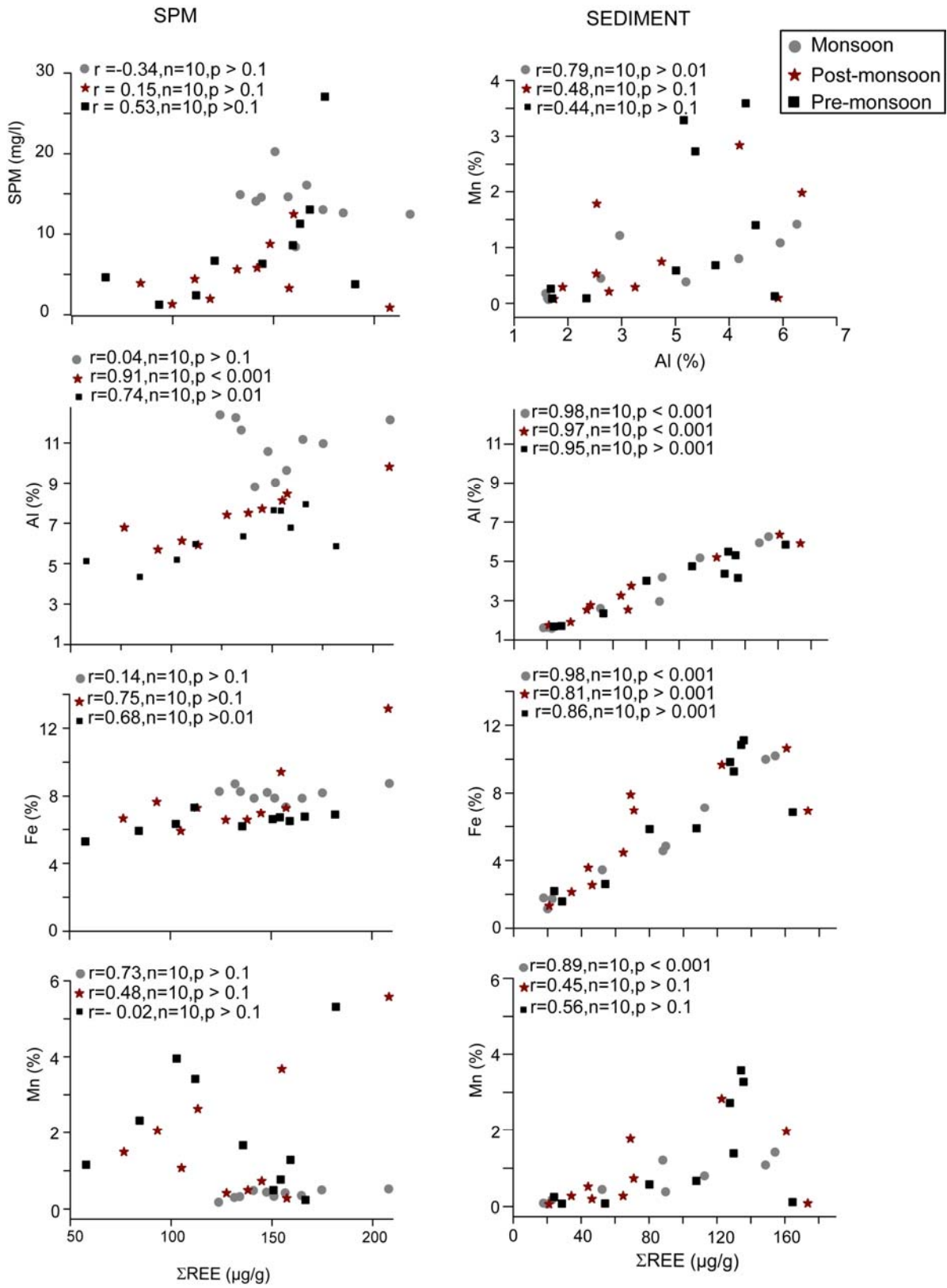


Figure. 4

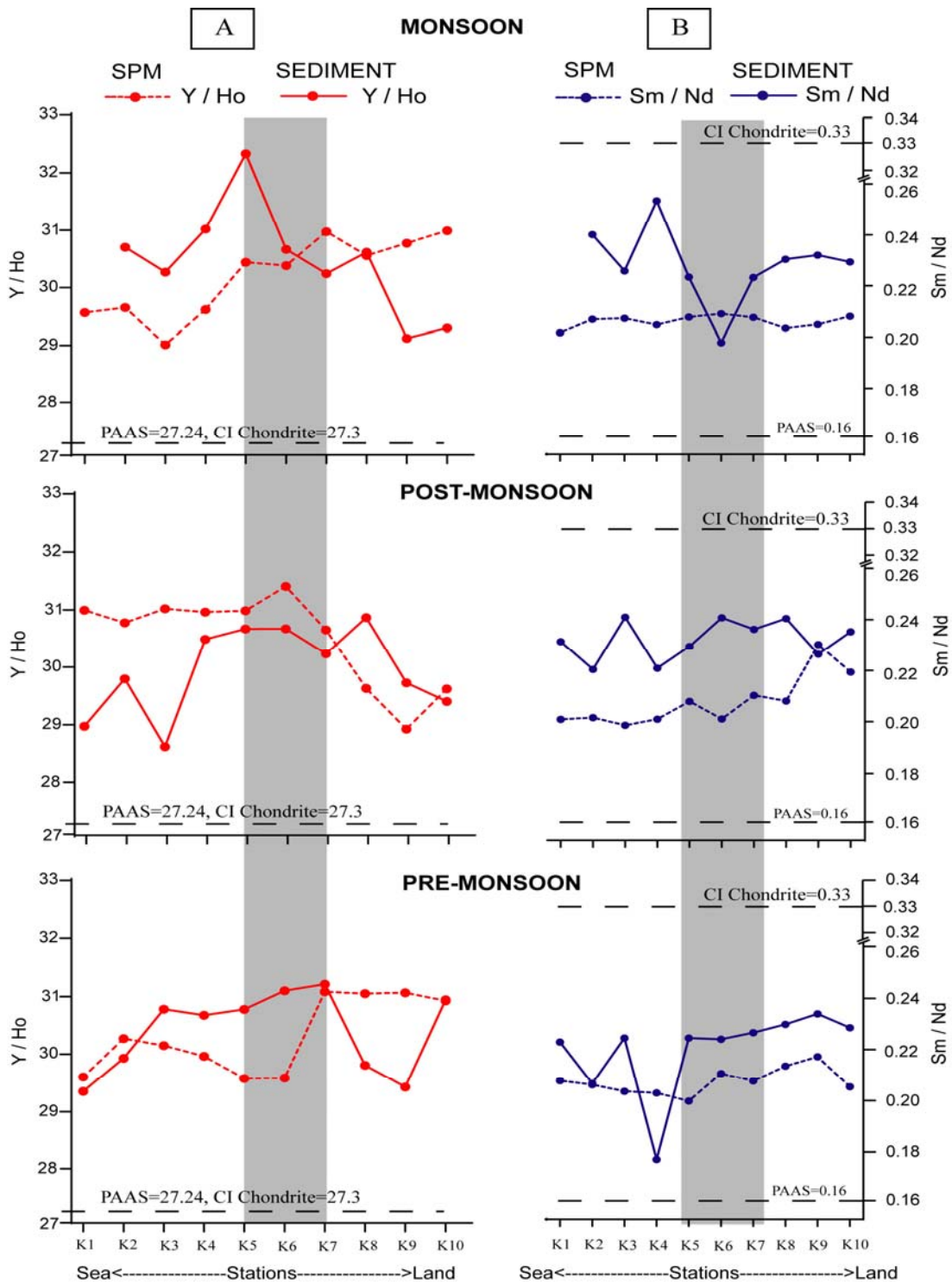


Figure. 5

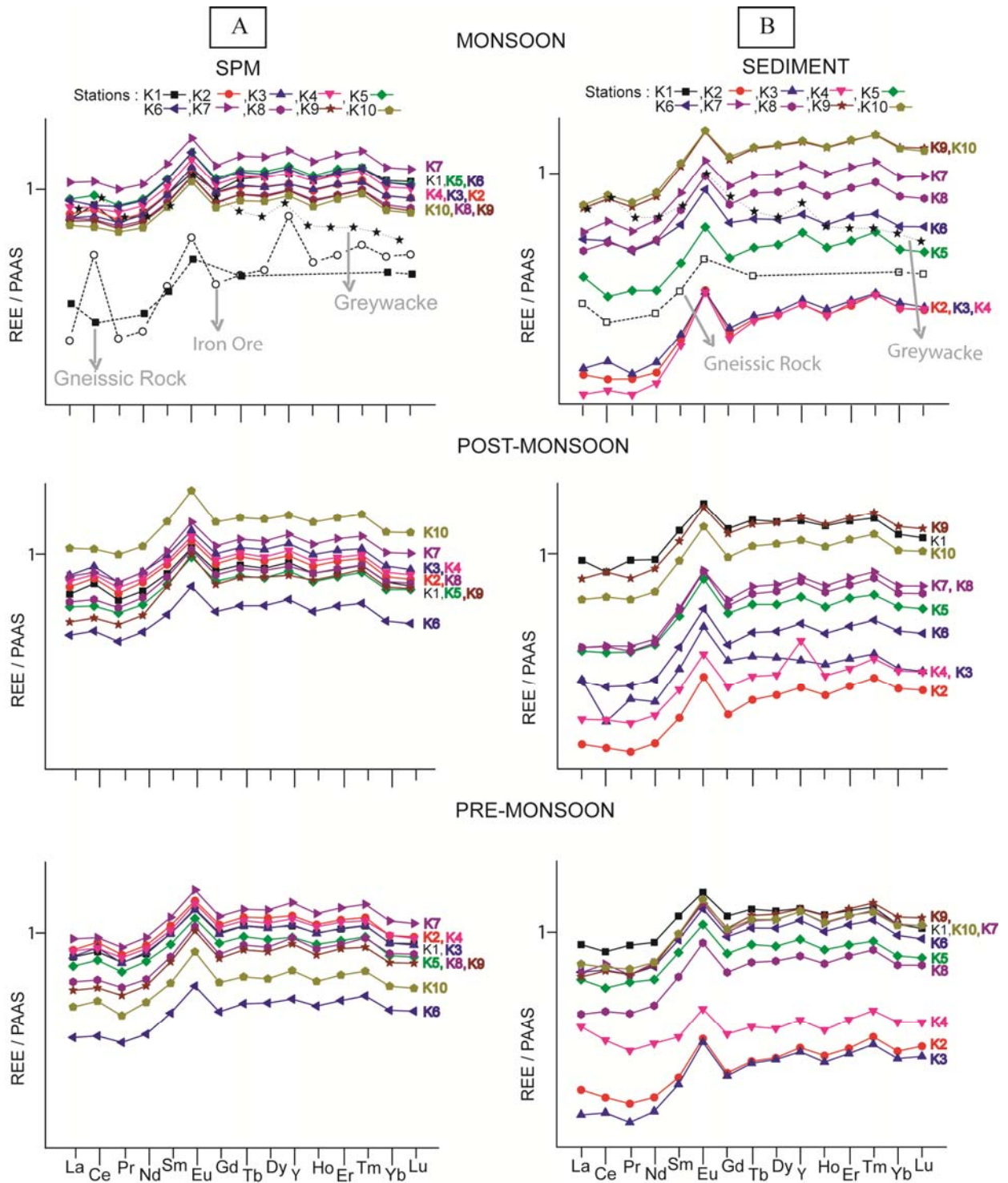


Figure. 6

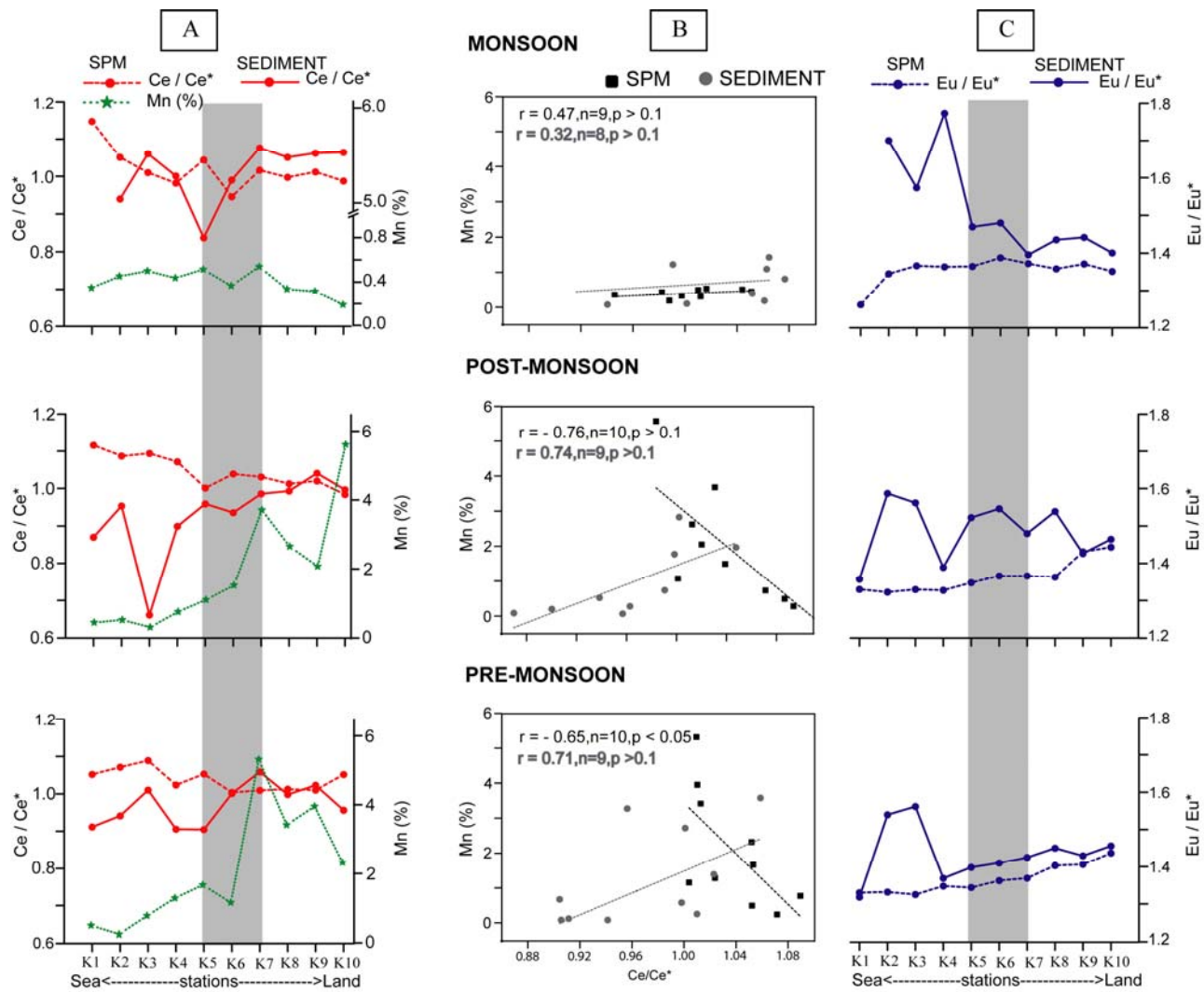


Figure. 7

Table 1: Analytical results of USGS Certified Reference of MAG-1 and observed values (mean of 2 analysis).

	USGS Certified Value		Present Study		Accuracy(%)	Precision(%)
	Mean	SD	Mean	SD	±	±
Al (%)	8.66	±0.16	8.28	±0.14	4.37	1.21
Fe (%)	4.58	±0.42	4.36	±0.07	4.71	1.15
Mn (%)	0.08	±0.42	0.07	±1.6	0.22	1.27
La	43	±4	43.10	±1.14	0.23	1.76
Ce	88	±9	88.02	±5.34	0.02	1.10
Pr	9.3		9.32	±0.30	0.20	2.61
Nd	38	±5	38.10	±1.51	0.26	1.84
Sm	7.5	±0.6	7.48	±0.06	0.29	3.01
Eu	1.55	±0.14	1.59	±0.02	2.35	0.12
Gd	5.8	±0.7	5.78	±0.09	0.35	1.83
Tb	0.96	±0.09	0.95	±0.02	0.99	0.30
Dy	5.2	±0.3	5.16	±0.09	0.72	2.40
Ho	1.02	±0.1	0.99	±0.02	2.79	2.96
Er	3		2.97	±0.09	1.08	1.22
Tm	0.43		0.43	±0.01	0.93	2.26
Yb	2.6	±0.3	2.57	±0.08	1.15	2.06
Lu	0.4	±0.04	0.39	±0.01	2.13	3.32
Y	28		28.07	±0.09	0.23	0.77

$$\text{Accuracy (\%)} = \left[\frac{\text{Mean} - \text{Certified value}}{\text{Certified value}} \right] \times 100 ; \text{Precision (\%)} = \left[\frac{\text{Measured 1} - \text{Measured 2}}{\text{Average}} \right] \times 100$$

Table : 2 Concentrations of SPM (mg/l), Al, Fe and Mn (%) and REE ($\mu\text{g/g}$) in suspended particulate matter in the Kali River Estuary.

Stations	Salinity	SPM	Al	Fe	Mn	La	Ce	Pr	Nd	Sm	Eu	Gd	Tb	Dy	Y	Ho	Er	Tm	Yb	Lu	Σ REE	LREE/HREE	LREE/MREE	Y/Ho	Sm/Nd	Ce/Ce*	Eu/Eu*
Monsoon																											
K 10	0.04	15.2	12.4	8.3	0.2	25.5	51.2	5.4	21.6	4.5	1.2	3.8	0.7	4.1	25.1	0.8	2.5	0.39	2.21	0.33	124	18.99	6.91	31.0	0.21	0.99	1.35
K 9	0.04	14.4	12.3	8.7	0.3	26.7	55.2	5.6	22.9	4.7	1.3	4.0	0.7	4.3	26.6	0.9	2.7	0.4	2.29	0.34	132	19.44	6.98	30.8	0.21	1.01	1.37
k 8	0.04	14.9	11.6	8.3	0.3	27.6	56.0	5.7	23.5	4.8	1.3	4.0	0.7	4.4	26.8	0.9	2.7	0.4	2.35	0.35	135	19.54	7.04	30.6	0.20	1.00	1.36
K 7	0.04	12.7	12.2	8.7	0.5	42.1	87.2	8.8	36.1	7.5	2.0	6.2	1.1	6.9	42.6	1.4	4.3	0.64	3.65	0.55	208	19.10	6.96	31.0	0.21	1.02	1.37
K 6	0.04	13.3	11.2	7.9	0.4	34.0	66.0	7.2	29.7	6.2	1.7	5.2	0.9	5.6	34.3	1.1	3.5	0.52	3.06	0.45	165	18.18	6.60	30.4	0.21	0.95	1.39
K 5	0.06	12.9	11.0	8.2	0.5	34.7	74.2	7.3	30.2	6.3	1.7	5.3	1.0	5.8	35.4	1.2	3.6	0.52	3.06	0.46	175	19.10	6.91	30.5	0.21	1.04	1.36
K 4	0.09	16.4	9.7	7.4	0.4	31.6	63.9	6.7	28.0	5.7	1.5	4.9	0.9	5.4	32.5	1.1	3.4	0.5	2.9	0.44	157	18.04	6.64	29.6	0.20	0.98	1.36
K 3	0.55	20.7	8.8	7.9	0.5	27.8	58.2	6.0	25.1	5.2	1.4	4.5	0.8	4.8	28.8	1.0	3.0	0.44	2.62	0.39	141	18.05	6.60	29.0	0.21	1.01	1.37
K 2	0.50	14.9	10.6	8.2	0.5	29.1	62.8	6.2	25.5	5.3	1.4	4.5	0.8	4.8	28.9	1.0	3.0	0.45	2.61	0.39	148	19.10	6.96	29.7	0.21	1.05	1.34
K 1	3.50	8.6	9.0	7.9	0.3	27.4	66.3	5.9	25.9	5.2	1.3	4.6	0.9	5.4	32.4	1.1	3.4	0.52	3.13	0.48	152	16.56	6.78	29.6	0.20	1.15	1.26
Mean	0.49	14.4	10.9	8.1	0.4	30.6	64.1	6.5	26.9	5.5	1.5	4.7	0.9	5.1	31.3	1.0	3.2	0.48	2.79	0.42	154	18.61	6.84	30.2	0.21	1.02	1.35
Postmonsoon																											
K 10	0.05	1.0	9.8	13.2	5.6	41.5	84.5	8.8	37.1	8.1	2.3	6.8	1.2	7.1	42.8	1.5	4.4	0.65	3.66	0.56	208	18.60	18.60	29.6	0.22	0.98	1.44
K 9	0.06	1.4	5.7	7.7	2.1	17.5	37.6	3.9	16.5	3.8	1.1	3.3	0.6	3.6	21.0	0.7	2.2	0.34	1.91	0.29	93	15.86	15.85	28.9	0.23	1.02	1.43
k 8	1.92	2.1	5.9	7.3	2.6	22.1	46.7	4.7	20.3	4.2	1.1	3.6	0.7	3.9	23.4	0.8	2.4	0.36	2.04	0.31	113	18.39	18.39	29.6	0.21	1.01	1.36
K 7	4.00	3.4	8.1	9.4	3.7	29.9	64.2	6.4	27.3	5.7	1.6	5.1	0.9	5.5	34.1	1.1	3.4	0.5	2.87	0.44	155	17.68	17.68	30.6	0.21	1.03	1.37
K 6	11.70	4.1	6.8	6.6	1.5	15.0	32.3	3.2	13.6	2.7	0.7	2.4	0.4	2.6	15.8	0.5	1.6	0.23	1.29	0.19	77	19.67	19.67	31.4	0.20	1.04	1.37
K 5	17.20	4.6	6.1	5.9	1.1	20.9	43.3	4.4	18.7	3.9	1.0	3.4	0.6	3.5	22.2	0.7	2.2	0.33	1.86	0.29	105	18.75	18.75	31.0	0.21	1.00	1.35
K 4	24.20	9.0	7.7	7.0	0.7	28.2	62.6	5.9	25.5	5.1	1.3	4.4	0.8	4.5	28.2	0.9	2.7	0.4	2.28	0.34	145	21.21	21.21	30.9	0.20	1.07	1.33
K 3	34.40	12.8	8.5	7.3	0.3	30.3	68.8	6.3	27.5	5.4	1.4	4.7	0.8	4.9	30.5	1.0	3.0	0.43	2.45	0.36	157	21.37	21.37	31.0	0.20	1.09	1.33
K 2	29.50	6.0	7.5	6.6	0.5	26.4	60.0	5.6	24.4	4.9	1.3	4.2	0.8	4.3	26.5	0.9	2.6	0.38	2.16	0.32	138	21.18	21.18	30.7	0.20	1.09	1.32
K 1	30.70	5.8	7.4	6.6	0.4	24.3	56.2	5.1	22.0	4.4	1.2	3.8	0.7	4.0	24.5	0.8	2.4	0.35	2.03	0.3	127	21.27	21.27	31.0	0.20	1.12	1.33
Mean	15.40	5.0	7.4	7.7	1.8	25.6	55.6	5.4	23.3	4.8	1.3	4.2	0.7	4.4	26.9	0.9	2.7	0.4	2.26	0.34	132	19.40	19.40	30.5	0.21	1.05	1.36
Premonsoon																											
K 10	0.06	1.3	4.3	5.9	2.3	16.3	35.7	3.3	15.0	3.1	0.9	2.6	0.5	2.7	17.4	0.6	1.7	0.26	1.51	0.23	84	18.84	6.83	30.9	0.21	1.05	1.44
K 9	1.63	2.5	5.2	6.3	4.0	19.8	41.8	4.2	18.2	4.0	1.1	3.5	0.6	3.8	23.8	0.8	2.4	0.34	1.99	0.3	103	16.79	6.14	31.1	0.22	1.01	1.41
k 8	3.94	6.9	6.0	7.3	3.4	21.9	45.9	4.7	19.7	4.2	1.2	3.6	0.7	4.0	25.5	0.8	2.5	0.38	2.22	0.34	112	16.95	6.37	31.0	0.21	1.01	1.4
K 7	7.22	3.9	5.9	6.9	5.3	36.2	75.3	7.5	32.1	6.7	1.8	5.7	1.0	6.1	38.6	1.2	3.8	0.57	3.25	0.48	182	18.61	6.71	31.1	0.21	1.01	1.37
K 6	9.71	4.8	5.1	5.3	1.2	11.3	23.6	2.4	10.3	2.2	0.6	1.8	0.3	2.1	12.4	0.4	1.3	0.19	1.14	0.17	58	17.03	6.43	29.6	0.21	1.00	1.36
K 5	12.90	6.5	6.3	6.2	1.7	26.3	57.8	5.6	24.3	4.9	1.3	4.1	0.7	4.3	25.6	0.9	2.6	0.39	2.16	0.33	136	20.80	7.03	29.6	0.20	1.05	1.35
K 4	19.30	13.4	6.8	6.5	1.3	31.4	66.6	6.6	28.2	5.7	1.5	5.0	0.9	5.3	31.9	1.1	3.2	0.47	2.74	0.41	159	19.40	6.84	30.0	0.20	1.02	1.35
K 3	26.10	11.6	7.6	6.7	0.8	29.5	67.0	6.2	27.0	5.5	1.4	4.6	0.8	4.9	29.7	1.0	3.0	0.44	2.51	0.38	154	20.48	7.09	30.1	0.20	1.09	1.33
K 2	34.90	27.7	7.9	6.8	0.2	31.9	71.3	6.8	29.3	6.0	1.6	5.1	0.9	5.6	33.1	1.1	3.3	0.49	2.74	0.41	167	20.01	6.84	30.3	0.21	1.07	1.33
K 1	30.10	8.9	7.6	6.6	0.5	29.3	64.0	6.2	26.5	5.5	1.4	4.7	0.8	5.0	29.4	1.0	3.0	0.44	2.51	0.38	151	19.95	6.83	29.6	0.21	1.05	1.33
Mean	14.60	8.8	6.3	6.5	2.1	25.4	54.9	5.4	23.1	4.8	1.3	4.1	0.7	4.4	26.7	0.9	2.7	0.4	2.28	0.34	130	18.89	6.71	30.3	0.21	1.04	1.37
PAAS ^a			10.0	4.5	0.1	38.2	79.6	8.8	33.9	5.6	1.1	4.7	0.8	4.7	27.0	1.0	2.9	0.4	2.8	0.4	185	24.69	8.97	27	0.16		
ASSWR ^b			8.7	5.8	0.2	37.4	73.6	8.0	32.2	6.1	1.3	5.3	0.8	4.3	21.9	0.9	2.2	0.4	2.1	0.4	175	29.65	8.08	24.9	0.19	0.97	1.07

LREE are La to Nd, MREE are Sm to Ho and HREE are Er to Lu (Rollinson, 1993).

^a PAAS : Post-Archaean Average Australian Shale (McLennan, 1989).

^b ASSWR : Average Suspended Sediment in World Rivers (Viers et al.,2009).

Table : 3 Concentrations of Al, Fe and Mn (%) and REE ($\mu\text{g/g}$) in bottom sediments of the Kali River Estuary.

Stations	Al	Fe	Mn	La	Ce	Pr	Nd	Sm	Eu	Gd	Tb	Dy	Y	Ho	Er	Tm	Yb	Lu	Σ REE	LREE/HREE	LREE/MREE	Y/Ho	Sm/Nd	Ce/Ce*	Eu/Eu*		
Monsoon																											
k 10	6.26	10.20	1.42	26.92	61.86	6.30	27.22	6.25	1.77	5.66	1.05	6.53	39.51	1.35	4.21	0.63	3.76	0.56	154.10	13.35	5.41	29.31	0.25	1.06	1.40		
K 9	5.95	10.00	1.09	25.97	59.28	5.99	25.91	6.01	1.76	5.46	1.04	6.46	38.98	1.34	4.16	0.64	3.82	0.58	148.40	12.73	5.31	29.13	0.23	1.06	1.44		
K 8	4.20	4.85	0.39	15.91	35.86	3.67	15.78	3.64	1.05	3.25	0.62	3.77	23.46	0.77	2.41	0.37	2.16	0.32	89.60	13.54	5.44	30.63	0.23	1.05	1.43		
K 7	5.18	7.13	0.80	19.70	45.71	4.52	19.83	4.43	1.25	4.04	0.76	4.65	29.71	0.98	3.07	0.46	2.71	0.42	112.50	13.48	5.57	30.25	0.15	1.08	1.39		
K 6	2.96	4.57	1.22	18.16	36.61	3.60	15.50	3.07	0.89	2.64	0.46	2.75	16.81	0.55	1.73	0.25	1.53	0.23	88.00	19.71	7.14	30.68	0.18	0.99	1.48		
K 5	2.61	3.45	0.45	11.81	19.30	2.29	8.82	1.97	0.58	1.76	0.33	2.05	13.65	0.42	1.31	0.21	1.17	0.18	52.20	14.74	5.93	32.35	0.17	0.84	1.47		
K 4	1.62	1.79	0.09	3.03	6.51	0.69	3.01	0.76	0.28	0.70	0.14	0.92	5.99	0.19	0.65	0.10	0.60	0.09	17.70	9.24	4.42	31.03	0.19	1.00	1.77		
K 3	1.59	1.74	0.18	4.09	9.12	0.87	3.85	0.87	0.28	0.79	0.15	0.96	6.30	0.21	0.66	0.10	0.64	0.09	22.70	12.02	5.52	30.28	0.20	1.06	1.57		
K 2	1.64	1.15	0.07	3.81	7.40	0.82	3.41	0.82	0.28	0.74	0.15	0.92	5.99	0.20	0.62	0.10	0.60	0.09	20.00	10.94	4.97	30.71	0.20	0.94	1.70		
K 1																											
Mean	3.56	4.99	0.63	14.38	31.29	3.19	13.70	3.09	0.90	2.78	0.52	3.22	20.04	0.67	2.09	0.32	1.89	0.28	78.36	13.31	5.52	30.49	0.23	1.01	1.52		
Postmonsoon																											
k 10	5.20	9.66	2.83	22.67	47.84	5.15	21.71	5.10	1.48	4.47	0.85	5.25	31.61	1.08	3.36	0.51	2.93	0.45	122.90	13.44	5.34	29.38	0.24	0.99	1.46		
K 9	6.36	10.64	1.97	28.85	64.20	6.61	28.42	6.43	1.87	5.91	1.10	6.74	41.70	1.40	4.36	0.66	3.88	0.58	161.00	13.51	5.46	29.70	0.23	1.04	1.43		
K 8	2.54	7.90	1.77	12.92	26.79	2.81	11.89	2.86	0.88	2.53	0.48	3.01	19.46	0.63	1.97	0.30	1.77	0.27	69.10	12.60	5.23	30.84	0.24	0.99	1.54		
K 7	3.75	6.96	0.73	12.91	27.00	2.99	12.44	2.94	0.89	2.71	0.53	3.26	20.51	0.68	2.15	0.33	1.93	0.30	71.00	11.77	5.03	30.21	0.24	0.98	1.48		
K 6	2.54	3.56	0.52	8.60	16.64	1.87	7.70	1.85	0.57	1.60	0.31	1.88	11.89	0.39	1.22	0.19	1.14	0.17	44.10	12.83	5.28	30.64	0.24	0.93	1.54		
K 5	3.26	4.46	0.28	12.37	24.96	2.78	11.64	2.67	0.80	2.32	0.43	2.58	16.27	0.53	1.69	0.25	1.52	0.23	64.80	14.04	5.54	30.64	0.23	0.96	1.52		
K 4	2.77	2.55	0.20	9.81	17.92	2.08	8.34	1.84	0.50	1.53	0.27	1.59	9.72	0.32	1.01	0.15	0.92	0.14	46.40	17.13	6.31	30.46	0.22	0.90	1.39		
K 3	1.91	2.13	0.28	8.82	11.05	1.60	5.95	1.43	0.46	1.33	0.23	1.38	7.72	0.27	0.83	0.13	0.73	0.11	34.30	15.26	5.37	28.54	0.24	0.66	1.56		
K 2	1.75	1.32	0.06	4.14	8.13	0.86	3.66	0.81	0.25	0.71	0.14	0.89	5.60	0.19	0.60	0.09	0.58	0.09	21.10	12.34	5.63	29.77	0.22	0.95	1.59		
K 1	5.92	6.93	0.08	35.85	64.17	8.17	31.63	7.31	1.95	6.26	1.15	6.82	39.83	1.38	4.19	0.62	3.55	0.52	173.60	15.75	5.62	28.95	0.23	0.87	1.36		
Mean	3.60	5.61	0.87	15.69	30.87	3.49	14.34	3.32	0.97	2.94	0.55	3.34	20.43	0.69	2.14	0.32	1.90	0.29	80.83	13.87	5.48	29.91	0.23	0.93	1.49		
Premonsoon																											
k 10	4.16	11.11	3.28	26.68	52.71	5.73	23.78	5.43	1.58	4.82	0.90	5.43	34.40	1.11	3.47	0.51	3.05	0.47	135.70	14.52	5.65	30.93	0.23	0.96	1.46		
K 9	5.50	9.28	1.39	22.96	50.57	5.37	23.03	5.39	1.56	4.87	0.94	5.78	35.45	1.21	3.75	0.57	3.37	0.51	129.90	12.43	5.16	29.42	0.23	1.02	1.43		
K 8	4.02	5.84	0.58	14.79	31.36	3.39	14.29	3.28	0.95	2.91	0.54	3.33	20.41	0.69	2.16	0.33	1.92	0.29	80.20	13.59	5.45	29.79	0.23	1.00	1.45		
K 7	5.31	10.84	3.58	24.18	54.61	5.35	23.64	5.36	1.51	4.66	0.89	5.41	34.39	1.10	3.44	0.52	3.10	0.47	134.20	14.31	5.70	31.21	0.23	1.04	1.43		
K 6	4.38	9.84	2.72	24.28	51.00	5.38	22.66	5.07	1.42	4.42	0.81	4.90	31.03	1.00	3.10	0.47	2.72	0.40	127.60	15.45	5.86	31.09	0.22	1.00	1.41		
K 5	4.75	5.90	0.67	22.27	41.33	4.91	19.46	4.37	1.18	3.62	0.67	3.97	24.80	0.81	2.46	0.36	2.14	0.32	107.90	16.68	6.02	30.77	0.22	0.90	1.40		
K 4	2.35	2.61	0.08	12.75	22.27	2.18	9.13	1.62	0.44	1.40	0.25	1.51	9.60	0.31	1.02	0.16	0.98	0.15	54.20	20.07	8.38	30.67	0.18	0.90	1.37		
K 3	1.69	2.20	0.25	4.52	9.50	0.94	4.11	0.92	0.30	0.86	0.17	1.04	6.59	0.21	0.68	0.11	0.64	0.10	24.10	12.52	5.46	30.77	0.22	1.01	1.56		
K 2	1.71	1.58	0.08	6.04	11.35	1.17	4.84	1.00	0.31	0.89	0.17	1.06	6.91	0.23	0.73	0.12	0.69	0.11	28.70	14.18	6.40	29.92	0.21	0.94	1.54		
K 1	5.85	6.86	0.12	33.56	63.30	7.58	30.08	6.70	1.72	5.64	1.01	6.00	35.62	1.21	3.67	0.54	3.09	0.45	164.60	17.34	6.03	29.34	0.22	0.91	1.32		
Mean	3.97	6.61	1.28	19.20	38.80	4.20	17.50	3.91	1.10	3.41	0.64	3.84	23.92	0.79	2.45	0.37	2.17	0.33	98.71	15.11	6.01	30.39	0.22	0.97	1.44		